Conformational Change Coupling the Dimerization and Activation of KSHV Protease†

Todd R. Pray,‡,⊥ K. Kinkead Reiling,‡ Berj G. Demirjian,§ and Charles S. Craik*,§

Graduate Group in Biophysics, Department of Pharmaceutical Chemistry and of Biochemistry and Biophysics, The University of California, San Francisco, California 94143

Received September 4, 2001; Revised Manuscript Received October 31, 2001

ABSTRACT: The mechanism of herpesviral protease activation upon dimerization was studied using two independent spectroscopic assays augmented by directed mutagenesis. Spectroscopic changes, attributable to dimer interface conformational plasticity, were observed upon dimerization of Kaposi's sarcoma-associated herpesvirus protease (KSHV Pr). KSHV Pr's dissociation constant of 585 ± 135 nM at 37 °C was measured by a concentration-dependent, 100-fold increase in specific activity to a value of 0.275 ± 0.023 μM product min^{-1} (μM enzyme)$^{-1}$. A 4 nm blue-shifted fluorescence emission spectrum and a 25% increase in ellipticity at 222 nm were detected by circular dichroism upon dimer association. This suggested enhanced hydrophobic packing within the dimer interface and/or core, as well as altered secondary structures. To better understand the structure−activity relationship between the monomer and the dimer, KSHV Pr molecules were engineered to remain monomeric via substitution of two separate residues within the dimer interface, L196 and M197. These mutants were proteolytically inactive while exhibiting the spectroscopic signature and thermal stability of wild type, dissociated monomers (T_M = 75 °C). KSHV Pr conformational changes were found to be relevant in vivo, as the autoproteolytic inactivation of KSHV Pr at its dimer disruption site [Pray et al. (1999) *J. Mol. Biol.* 289, 197−203] was detected in viral particles from KSHV-infected cells. This characterization of structural plasticity suggests that the structure of the KSHV Pr monomer is stable and significantly different from its structure in the dimer. This structural uniqueness should be considered in the development of compounds targeting the dimer interface of KSHV Pr monomers.

The completely sequenced human herpesvirus 8 (HHV-8)[1] (*1*), also known as Kaposi's sarcoma-associated herpesvirus (KSHV), is the sexually transmitted, etiological agent for Kaposi's sarcoma (KS), one of the most common AIDS-associated malignancies (reviewed in ref *2*). An enzyme essential to the propagation of all herpesviruses, expressed as a late gene product during lytic viral replication, is each virus's maturational protease (reviewed in refs *3* and *4*). These serine proteases process the capsid's scaffolding, composed of roughly 10^3 assembly protein (AP) molecules, at conserved cleavage sites, liberating them from the interior of the viral procapsid to allow packaging of the virus's DNA. The crystal structures of the proteases from KSHV (*5*), human cytomegalovirus (hCMV) (*6*−*9*), Varicella Zoster virus (VZV) (*10*), and herpes simplex virus-1 and -2 (HSV-1 and -2) (*11*) characterize this class of dimeric enzymes' novel fold, the two structurally distinct Ser−His−His active sites of the homodimer, and the conformation of the monomer−monomer interaction surface.

Oligomerization for a variety of proteases has been observed, and structural models of the linkage between quaternary state and enzymatic activity are beginning to emerge for a number of these enzymes. For example, calpain's catalytic and regulatory subunits heterodimerize and then undergo activating conformational rearrangement upon Ca^{2+} binding (*12*). In addition, bleomycin hydrolase exhibits dimer and hexamer formation (*13*), and tryptase—a heparin-stabilized tetramer—has been shown to undergo activating conformational changes during association (reviewed in ref *14*). Even higher order assemblies are exhibited by tricorn protease (*15*) and the proteasome, which function as supermolecular proteolytic machines. In the case of the proteasome, oligomerization has been demonstrated to induce autocatalytic activation (*16*). Perhaps the best-understood, and most intuitive, case of an activating oligomerization event in a proteolytic enzyme occurs for the retroviral proteases. These enzymes, such as the one encoded by HIV,

† Research was supported by the NIH (C.S.C., GM56531). K.K.R. and T.R.P. were partially supported by a graduate training grant (NIH GM08204) and by the ARCS Foundation. B.G.D. was supported in part by the UCSF Summer Research Training Program.

* To whom correspondence should be addressed. Charles S. Craik: phone: 415-476-8146; fax: 415-502-8298; e-mail craik@cgl.ucsf.edu.

‡ Graduate Group in Biophysics.

§ Department of Pharmaceutical Chemistry and of Biochemistry and Biophysics.

⊥ Present address: Dept. of Combinatorial Biology, Rigel Pharmaceuticals, Inc., 240 East Grand Ave., South San Francisco, CA 94080.

[1] Abbreviations: KSHV Pr, Kaposi's sarcoma-associated herpesvirus protease; KS, Kaposi's sarcoma; HIV, human immunodeficiency virus; HSV, herpes simplex virus; VZV, Varicella-zoster virus; hCMV, human cytomegalovirus; EBV, Epstein−Barr virus; Pr/AP, protease-assembly protein; AP, assembly protein; CD, circular dichroism; TPA, 12-*O*-tetradecanoylphorbol 13-acetate; D-site, dimer disruption site; R-site, release site; DMF, dimethyl formamide.

10.1021/bi011753g CCC: $22.00
Published on Web 01/10/2002

construct a single, shared active site at their dimer interface (*17*, *18*). The variation in detail and the conservation of the activation phenotype across protease families indicate that allosteric switching for proteases is a commonly seen, but diversely executed, process in nature.

Herpesviral proteases, which present two structurally and spatially distinct active sites, likely depend on dimer-interface-induced changes to transmit oligomeric state information to the catalytic residues. Our detection of a dimer disrupting cleavage site (D-site) within the dimer interface of KSHV Pr, cleavage at which *in*activates the enzyme, highlights one path of interface-dependent regulation (*19*). This cleavage after residue Ala203 ushers in structural differences between active KSHV Pr dimers and the 203 amino acid, truncated KSHV Pr (KSHV Pr Δ). KSHV Pr Δ contains only 60% of the full-length molecule's α-helical content. The HCMV protease has also been shown to undergo conformational changes in the presence of solvent additives and/or inhibitor binding. Spectroscopic assays (*20*) and X-ray crystallography (*21*) have provided evidence that many of these changes involve the dimer interface. These findings have led to the hypothesis that dimerization may be a determinant of the structure of these enzymes affecting their activity; a proposal in agreement with biochemical data demonstrating the stimulation of hCMV and HSV Pr specific activity as dimers assemble in solution (*22*, *23*). In effect, oligomerization of these molecules, and the concomitant ordering of their active sites and/or substrate binding determinants, could serve as a zymogen activation switch, distinct from, but analogous to, the regulatory strategies utilized by other classes of proteases (reviewed in ref *24*).

In this study, we provide the first direct structural evidence to support the hypothesis that herpesviral proteases undergo activating conformational changes upon dimerization itself. Through the use of sensitive spectroscopic probes of the secondary and tertiary structure of KSHV Pr, we observed substrate-independent conformational switching upon monomer−monomer association. This switching correlates precisely with the protease's activation profile, as observed by its concentration- and temperature-dependent specific activity profiles. These dimerization dependent structural transitions have been specifically blocked by site-directed mutagenesis of two critical amino acid residues within KSHV Pr's dimer interface, L196 and M197. These point mutations eliminate dimerization and abrogate cleavage of synthetic peptide substrates by the altered KSHV Pr monomers. In addition, we detected the autolysis at the D-site (*19*) within the dimer interface of KSHV Pr during lytic viral replication, indicating that the enzyme undergoes proteolytic inactivation in vivo. The detection of both full-length KSHV Pr and KSHV Pr Δ in viral capsid particles suggests that the different secondary, tertiary, and quaternary structural states observed in this biochemical study occur during the KSHV life cycle.

EXPERIMENTAL PROCEDURES

Protein Purification. KSHV Pr variants were expressed in *Escherichia coli* and purified as described previously (*19*). The total protein concentration of purified samples was determined by measuring their absorbance at 280 nm using a calculated ϵ_{280} of 0.9 mL mg^{-1} cm^{-1}, after dilution into 8 M GuHCl to avoid any differences in absorbance between monomeric and dimeric protease molecules.

Virus/Capsid Isolation. BCBL-1 cells were cultured essentially as described (*25*). Late gene expression and lytic replication were induced by the addition of 12-*O*-tetradecanoylphorbol 13-acetate (TPA) to a concentration of 20 ng/mL. The cultures were then grown for an additional 6 days. To harvest the media supernatant containing virus particles as well as any immature nucleocapsids released upon cell lysis, cells were pelleted by centrifugation at 1500 rpm for 10 min at 4 °C in a Beckman tabletop tissue culture centrifuge. The supernatant was decanted and spun again at 2500 rpm for 10 min at 4 °C. To isolate viral and capsid particles, this cleared media was spun in an SW-28 rotor at 15 000 rpm for 2 h at 4 °C. Following centrifugation, the media was gently aspirated, and the pellets from all tubes were resuspended in a total volume of 200 μL of 1× SDS−PAGE loading buffer and frozen at −75 °C until further analysis could be performed.

Kinetic Assays. KSHV Pr activity assays were performed using a synthetic oligopeptide substrate containing a fluorescence donor-quencher pair flanking the native KSHV R-site sequence, YLKA-SQFP (*19*). The assay buffer contained 0.7 M potassium phosphate (pH 8), 150 mM KCl, 25% (vol/vol) glycerol, 0.1 mM EDTA, and 1 mM β-mercaptoethanol. Assays were monitored and performed as described (*19*), at the conditions indicated in the text and figure legends. The substrate was stored as a 2.5 mM stock in dimethylformamide (DMF), and the concentration of DMF was kept constant in all assays at 0.8% (vol/vol). The total concentration of substrate in all assays was kept at or below 20 μM to avoid the inner-filter effect (*26*). k_{cat} and K_M were determined by increasing the substrate concentration from the low nanomolar range to 20 μM at a constant enzyme concentration of 100 nM. On the basis of the above measurements and in agreement with previous studies, the lower threshold for detection of product formation by this assay is 2.4×10^{-5} μM product/min (*19*). Data were analyzed by the Michaelis−Menten equation using nonlinear least-squares fitting within the Scientist software package (Micromath, Inc.).

To determine the K_d and maximum specific activity, A_{max}, for KSHV Pr in kinetic assays, the measured specific activity, A_{spec}, at experimental enzyme concentrations was related to the dimerization equilibrium using the following expression using the Scientist software package (Micromath, Inc.):

$$A_{spec} = A_{max} \frac{[Pr_2]}{[Pr] + [Pr_2]}$$

where [Pr] represents the concentration of free monomers in solution, and [Pr_2] is the concentration of KSHV Pr dimers. [Pr_2] is derived from [Pr] using the expressions:

$$[Pr_2] = \frac{[Pr]^2}{K_d}$$

and:

$$[Pr] = \frac{\sqrt{1 + 8\frac{E_{tot}}{K_d}} - 1}{4/K_d}$$

which is derived, using the quadratic formula, from the following expression:

$$2\frac{[\mathrm{Pr}]^2}{K_\mathrm{d}} + [\mathrm{Pr}] - E_\mathrm{tot} = 0$$

where E_{tot} is the total experimental KSHV Pr monomer concentration (i.e., $[Pr] + 2[Pr_2]$).

Site-Directed Mutagenesis. Mutations encoding the amino acid substitutions L196A, M197D, and M197K were introduced into the KSHV Pr gene by PCR-mediated overlap extension as described previously for S204G and S114A mutations of this protease (*19*). The mutant codons were flanked upstream and downstream by four wild-type codons. The integrity of the KSHV Pr ORF and the mutations were verified by DNA sequencing.

Spectroscopy. CD and fluorescence emission spectroscopy were performed essentially as described (*19*). CD scans were performed on a Jasco 710 instrument in 1- or 0.2-cm temperature-controlled quartz cuvettes. Mean molar residue ellipticities were obtained after solvent spectrum subtraction and 15-fold signal averaging. Fluorescence emission scans were performed on a JY-SPEX Fluorolog-3 instrument. The excitation wavelength was 275 nm, and scans were solvent corrected and 10-fold averaged. Emission intensity was normalized to lamp strength (which varied no more than 1%) to yield fluorescence units of cps/μA. Peak positions of fluorescence emission profiles were determined using the GRAMS software provided by JY-SPEX.

Solvent Accessibility Measurements. Solvent accessibility was determined by the double cubic lattice method as implemented in the ASC software routine (*27*) using the structure of KSHV Pr (PDB accession code 1FL1) with solvent removed. Removing the uninterrogated monomer without any relaxation of the structure generated an approximation of the free monomer's surface area.

RESULTS

Activation of KSHV Pr upon Dimerization. To examine the functional role of dimerization for KSHV Pr, a study was undertaken of the concentration dependence of the enzyme's specific activity. To achieve the precision required by these measurements, the assay conditions were optimized to maximize enzyme activity. This enhancement was accomplished by increasing the phosphate buffer's concentration from 50 to 700 mM and the pH of the buffer medium from 7.0 to 8.0. Analogous conditions were used in previous studies to enhance the activity of hCMV and HSV-1 proteases (*22*, *28*). The k_{cat}/K_M value for 100 nM KSHV Pr in cleaving its R-site sequence under these new conditions was markedly increased to 2.2×10^4 M^{-1} min^{-1}, with a K_M of 2.9 ± 1.3 μM and a k_{cat} of 0.064 ± 0.01 min^{-1} at 20 °C. This specificity constant is over 40-fold higher than the value found previously for this enzyme for hydrolysis of this substrate, 500 M^{-1} min^{-1} (*19*). Under earlier KSHV Pr assay conditions, substrate saturation was never reached, and k_{cat} and K_M were not resolvable from the observed k_{cat}/K_M value (*19*, *29*). These new cosolvent conditions are in agreement with data on other herpesviral proteases, all of which required cosolvents for maximal activity and allowed the dimerization and activation studies in this report to be performed.

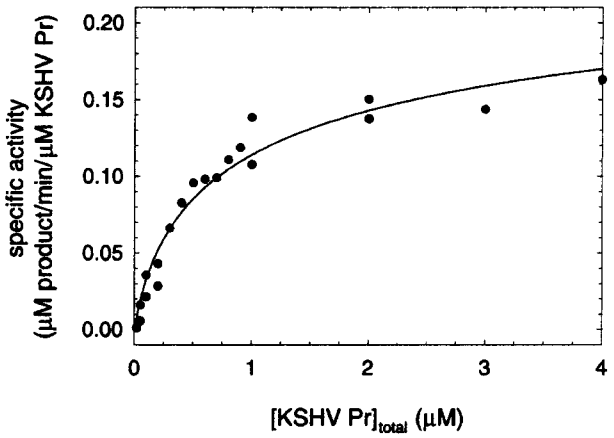

FIGURE 1: Stimulation of KSHV Pr specific activity upon dimerization. Plot of specific activity ([product] formed min^{-1} (μM total enzyme monomer)$^{-1}$) vs total enzyme monomer concentration (circles). Assays were performed at 37 °C in 500 μL quartz cuvettes with 20 μM total KSHV Pr M-site substrate and between 20 nM and 4 μM total enzyme. The best fit K_d of 585 ± 150 nM and maximum specific activity of 0.275 ± 0.023 μM product min^{-1} (μM enzyme)$^{-1}$, shown by the solid line, was obtained by simultaneously fitting two independent data sets.

KSHV Pr exhibited a nonlinear enhancement of specific activity with increasing total protein concentration at physiological temperature, 37 °C (Figure 1). At low total monomer concentrations, in the 20 nM range, KSHV Pr had minimal, but detectable specific activity of 0.0012 μM product (min)$^{-1}$ (μM enzyme)$^{-1}$. As the concentration of KSHV Pr was increased to the low micromolar range in the presence of constant, nearly saturating substrate levels (20 μM), a large stimulation of product turnover was observed. This enhancement reached a plateau for enzyme specific activity of 0.15 μM product (min)$^{-1}$ μM^{-1}, which represents a greater than 100-fold stimulation of product turnover. This activation of KSHV Pr as a function of its concentration was modeled, attributing the full specific activity of KSHV Pr directly to the free dimers in solution (see Experimental Procedures), similar to methods described previously for the related proteases from hCMV and HSV-1 (*22*, *23*). This analysis yielded a K_d of 585 ± 135 nM for two independent but simultaneously analyzed data sets and was shown to agree well with the experimental data (solid line in Figure 1). This K_d value is 3-fold lower than the 1.7 ± 0.9 μM previously observed for KSHV Pr under other, nonoptimal assay conditions (*19*), consistent with the modulation of the dimerization affinity of HSV-1 and hCMV Pr molecules under varied solution conditions (reviewed in ref *31*).

While activity is dependent upon dimerization for herpesviral proteases, it appears that, at least for the case of KSHV Pr, this is not due to the coupled activity of the dimer's two active sites. In mixing experiments with active KSHV Pr S204G ($\sim$500 nM to $\sim$10 μM) and inactive KSHV Pr S204G/S114A monomers (*19*), no detectable diminution of KSHV Pr S204G specific activity was observed, even at 10- to 100-fold molar excesses of the S204G/S114A variant after overnight, room temperature, or 4 °C incubations (unpublished observations). Under these conditions, where heterodimer formation should predominate over KSHV Pr S204G homodimer assembly, any effect of an inactive catalytic triad upon its dimer mate's active site would have been evident.

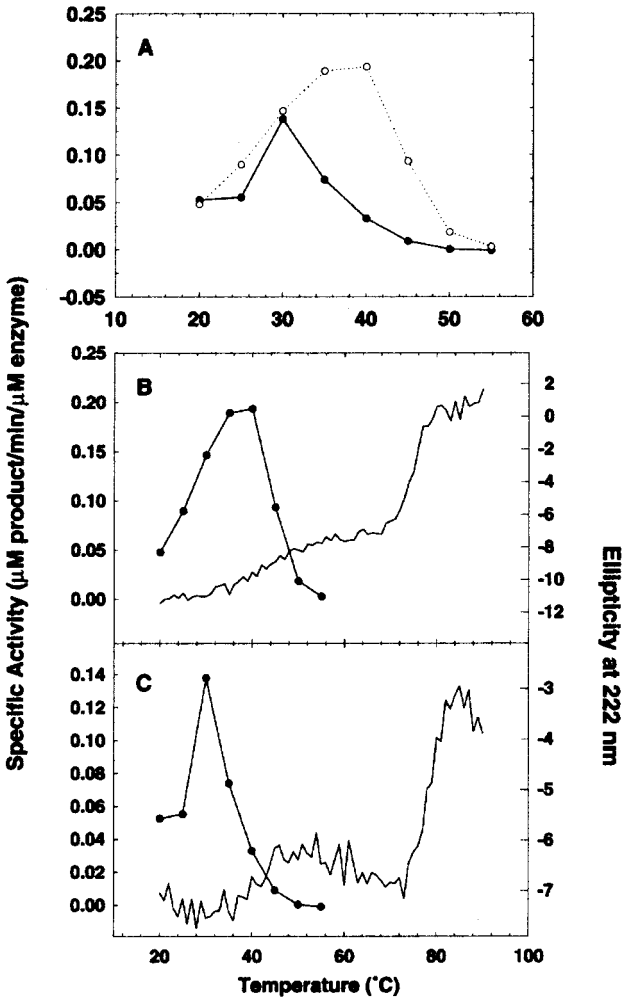

FIGURE 2: Linkage between structural changes and KSHV Pr's dimerization-enhanced activity. (A) Overlay of specific activity of 250 nM (filled circles) and 2.5 μM (open circles) KSHV Pr against cleavage of 20 μM KSHV Pr M-site substrate. (B) 2.5 μM KSHV Pr temperature−activity profile from panel A (solid circles), overlaid with the enzyme's temperature-dependent change in secondary structure detected by circular dichroism spectroscopy (line). (C) The same experiment done with 250 nM KSHV Pr (data from panel A), demonstrating the concentration-dependent increase in activity and stability of the enzyme.

Alteration of KSHV Pr Structure and Activity upon Dimer Dissociation. While the stimulation of catalytic activity upon dimerization for herpesviral proteases has been confirmed here for KSHV Pr, and elsewhere for related enzymes (*30*; reviewed in ref *31*), the structural basis for this has not been addressed experimentally. To begin to characterize any structural transitions affecting KSHV Pr activity upon dimer dissociation, the temperature dependencies of its spectral characteristics and specific activity were measured (Figure 2). At a concentration of 2.5 μM (roughly 5-fold above the enzyme's K_d at 37 °C, 585 nM), the specific activity of KSHV Pr increased 6-fold with temperature from 20 to 40 °C, then declined rapidly above 40 °C (Figure 2A). This loss of activity was congruent with a temperature-dependent loss in the enzyme's ellipticity at 222 nm detected by CD spectroscopy, in the absence of substrate (Figure 2B). In stark contrast to the 2.5 μM protease sample, the activity of 250 nM KSHV Pr increased only to 30 °C, and then decreased even more precipitously than the 2.5 μM protease sample to nearly undetectable levels (Figure 2A). The loss in CD, as a function of temperature, also paralleled the deactivation of the enzyme at the lower concentration (Figure 2C). The 3-fold increase in activity between 20 and 30 °C for both the 250 nM and 2.5 μM KSHV Pr samples agreed very well with transition state theory, which predicts a 3-fold rate enhancement for every 10 °C temperature rise (*32*).

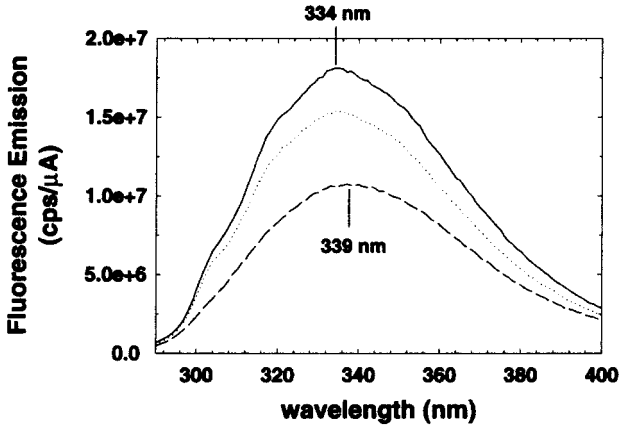

FIGURE 3: Temperature dependence of the fluorescence emission spectrum of KSHV Pr. 2.5 μM KSHV Pr was incubated in assay buffer at the indicated temperatures, and the intrinsic fluorescence emission was excited at a wavelength of 275 nm (20 °C, solid; 37 °C, dotted; 55 °C, dashed). The changes in shape and peak emission wavelength of the spectrum indicate possible tertiary structural changes and/or an overall increase in the solvent exposure of the partially buried aromatic residues within the enzyme upon dimer dissociation (see Figure 4A for a presentation of the crystal structure of KSHV Pr).

The coincidence of activity loss with a change in CD absorption, a sensitive measure of protein secondary structure, presented two possibilities: the change in ellipticity was due to a structural perturbation in the intact dimer, or to dissociation of the dimer and consequent alterations in monomer structure. The concentration dependence of the activity and structural transitions found in this study at intermediate temperatures implicated dimerization in this process. In addition, it was observed that the high-temperature loss in CD signal was insensitive to protease concentration with apparent T_M values of 75 °C, and likely resulted from the global unfolding of dissociated monomers. The transition, however, was irreversible, and the protein samples visibly precipitated upon cooling. Thus, the thermodynamic properties of KSHV Pr monomer stability were not quantitatable under these conditions.

A second, independent, spectroscopic assay of KSHV Pr structure monitored the intrinsic fluorescence emission of the enzyme as a function of temperature. Alterations in fluorescence emission intensity and spectral shape were detected that coincided with the loss of activity at the dissociation temperature regime identified in the activity and CD profiles (Figure 3). The decrease in fluorescence intensity, in part, may be due to the effect of elevated temperature upon fluorophore emission (*33*). However, the loss of the shoulders below 320 nm, and the shift in peak emission wavelength from 334 to 339 nm, both pointed to the possibility that the environment of emitting moieties within the protein is somewhat more solvent-accessible in the KSHV Pr monomer. This change in spectral profile was attributable to the Trp residues of KSHV Pr at positions 54, 109, and 156. The shift of the entire spectrum implies that

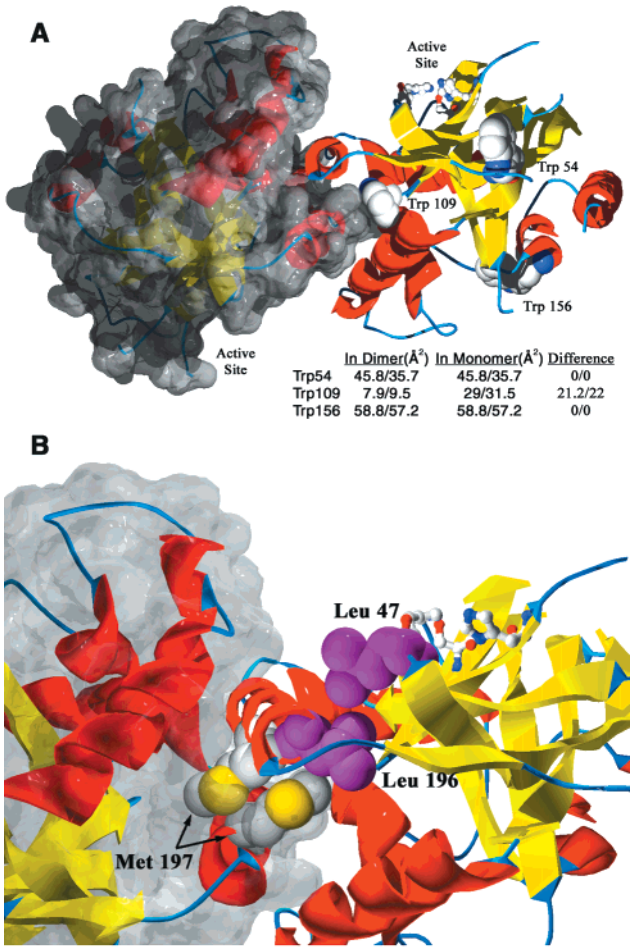

	In Dimer(Å²)	In Monomer(Å²)	Difference
Trp54	45.8/35.7	45.8/35.7	0/0
Trp109	7.9/9.5	29/31.5	21.2/22
Trp156	58.8/57.2	58.8/57.2	0/0

FIGURE 4: (A) Structure of KSHV Pr dimer is shown (*5*). The two active sites are labeled, as are the positions of the three Trp residues present near the surface of each monomer. Listed in the table are solvent accessibility values calculated for these three Trp residues in the context of the monomer and the dimer, demonstrating the large changes in environment possible for Trp109, in particular, upon dimerization. (B) Dimer interface residues chosen for substitution to test the role of oligomerization and structural changes for KSHV Pr are presented. The residue L196, which is absolutely conserved among herpesviral proteases and is in indirect contact with the catalytic H46 via L47, was substituted with an Ala. The residue M197, which makes intimate dimer-mate contacts, was substituted with the charged residues Lys or Asp.

the environments of all three Trp's were altered during the monomer−dimer transition. Trp54 and Trp156 are both partially buried near the surface of the enzyme's hydrophobic core and distant from the dimer interface of KSHV Pr (Figure 4A). Trp109, in contrast, is located within the dimer interface (Figure 4A). Thus, this residue likely underwent a fundamental change in environment upon dimer dissociation and interface remodeling.

Selective Perturbation of Dimerization and Activity by Dimer Interface Mutagenesis. Site-directed mutagenesis of the KSHV Pr dimer interface was employed to further elucidate the structure−function determinants linking dimerization and activity. It has previously been shown that the S204G dimer interface substitution at the D-site of KSHV Pr does not perturb dimerization or proteolytic activity (*19*). The ability to substitute this residue without conferring any measurable conformational change upon KSHV Pr demonstrates that the structural and functional linkage between the dimer interface and active sites of KSHV Pr does not exhibit

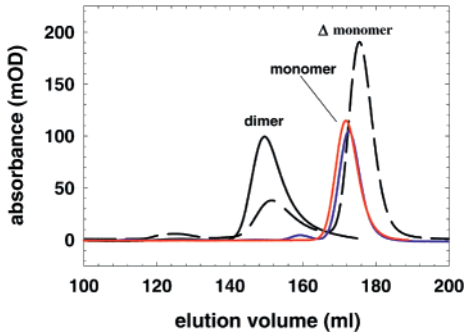

FIGURE 5: Perturbation of dimerization of KSHV Pr by point mutations within its dimer interface. Gel-filtration chromatography shows the loss of detectable dimerization at 0.1 mM of KSHV Pr upon introduction of the point mutations L196A or M197D. In solid black is the active, dimeric ~0.1 mM KSHV Pr S204G. In dashed black is ~0.2 mM wild-type KSHV Pr showing full-length dimers eluting with KSHV Pr S204G, as well as KSHV Pr Δ eluting at a monomer molecular weight. In solid red is ~0.1 mM KSHV Pr S204G/L196A, and in solid blue is ~0.1 mM KSHV Pr S204G/M197D. KSHV Pr S204G/M197K also exhibited only monomeric elution from the Superdex-75 column (not shown).

wholesale intolerance to dimer interface perturbation. In the current study, this fact was employed in an attempt to find specific mutations that abrogate enzyme activity by disrupting its dimerization.

Residues L196 and M197 were chosen for mutagenesis of the dimer interface. These adjacent amino acids are largely buried within the molecule's dimer interface (Figure 4). While L196 interacts mainly with residues from the same monomer, M197 makes intimate intermonomer contacts, both with neighboring residues and with the dimer mate's M197 amino acid side chain (*5*). L196 was substituted with Ala, yielding L196A, to examine the role of this side chain's hydrophobic interactions with neighboring residues in the same monomer. M197, which contributes roughly 120 Å, or 10%, of the surface area buried in the dimer interface by each monomer, was substituted with either Lys or Asp to create M197K and M197D. These M197 mutations were predicted to alter the enzyme's ability to homodimerize due to the introduction of like charges within a strongly self-associating region in the enzyme's dimer interface. All three mutations, L196A, M197D, and M197K, were introduced in the context of the previously characterized, stabilizing D-site S204G substitution to minimize KSHV Pr autolysis if the enzyme variants were proteolytically active (*19*).

Initial expression and purification trials for these dimer interface variants indicated phenotypic differences between the L196A, M197D, and M197K proteins and the dimeric, active KSHV Pr S204G enzyme. All three of the substituted proteases expressed well in the *E. coli* system developed for KSHV Pr S204G. The M197K variant protease, however, exhibited degradation, which resulted in a lower yield of full-length protein (not shown). All KSHV Pr variants were purified using the protocol developed for KSHV Pr S204G. The three double mutants behaved similarly to KSHV Pr S204G during hydrophobic and anion exchange separation (not shown). In contrast, size-exclusion of these samples over a Superdex-75 26/60 column (Pharmacia), at loading concentrations of 2−3 mg/mL (roughly 100 μM), where KSHV Pr S204G dimers readily form (*19*), indicated a loss of detectable dimerization (Figure 5). The monomers of L196A,

M197D, and M197K eluted slightly earlier than the 22 kD autolytic truncation product, KSHV Pr Δ, consistent with the higher molecular weight, 25 kD, of the full-length molecule. The propensity of these modified KSHV Pr monomers to aggregate at higher concentrations after purification, measured by dynamic light scattering (not shown), prevented the quantitation of possible low affinity dimerization by these variants over a broader concentration range.

The inability of these engineered KSHV Pr monomers to dimerize, in this assay, was associated with a complete loss in detectable proteolytic activity. Using the same synthetic oligopeptide, the KSHV Pr R-site substrate, and assay conditions used to characterize the activity of KSHV Pr S204G, no product formation greater than 2.4×10^{-5} μM product/min (see Methods) was observed even at protein concentrations as high as 10 μM for the L196A, M197D, and M197K variants. In addition, mixtures of M197D- and M197K-containing KSHV Pr molecules, a heterodimer of which would contain an attractive charge pair within the interface, did not produce any proteolytic activity. Further, addition of any three of the dimer interface variants developed in this study to active, dimeric KSHV Pr S204G at a 10- to 100-fold stoichiometric excess did not inhibit the activity of the enzyme, even after overnight room temperature or 4 °C incubations (unpublished observations). While the inactivity of these monomeric dimer interface variants was consistent with the stimulated activity of KSHV Pr S204G, HCMV, and HSV-1 dimers (*22*, *23*), the possibility existed that it could have been due to alterations in the overall structure or stability of the mutant KSHV Pr monomers and thus unrelated to their oligomeric state.

Dimer Interface KSHV Pr Mutants Retain Near-Native Monomer Structural Properties. To examine whether these M197 and L196 variant monomers maintained the structural characteristics of the active KSHV Pr S204G molecule, the same spectroscopic assays were used to examine the engineered monomers as had been applied to characterize the monomer−dimer transition of KSHV Pr S204G. First, the temperature dependencies of the CD at 222 nm for the dimer interface variant KSHV Pr molecules were recorded. All three KSHV Pr S204G variants—M197D, M197K, and L196A—lacked any concentration dependent loss in ellipticity at dimer dissociation temperatures (30−40 °C), and exhibited only a single, concentration-independent transition at the denaturation temperature, 75 °C, of KSHV Pr S204G monomers (Figure 6A). This indicated that the apparent global stability of dissociated monomers of both active, dimerization-competent S204G molecules, and the inactive dimer-interface mutants, were identical under these conditions. The magnitude of the mean molar residue ellipticity at 222 nm for all KSHV Pr monomers in this experiment was essentially identical, indicating that their helical contents were similar. Thus, the M197 and L196 mutations did not perturb detectably the global stability or secondary-structure content of the KSHV Pr monomer.

To further probe the structure of the dimer interface variants, and to see if the identical stabilities of the mutants indeed arose from similar secondary structures, full CD absorption spectra were recorded as a function of temperature. Wavelength scans, from 200 to 250 nm, of the M197D and L196A mutants at 20 °C indicated that the monomeric,

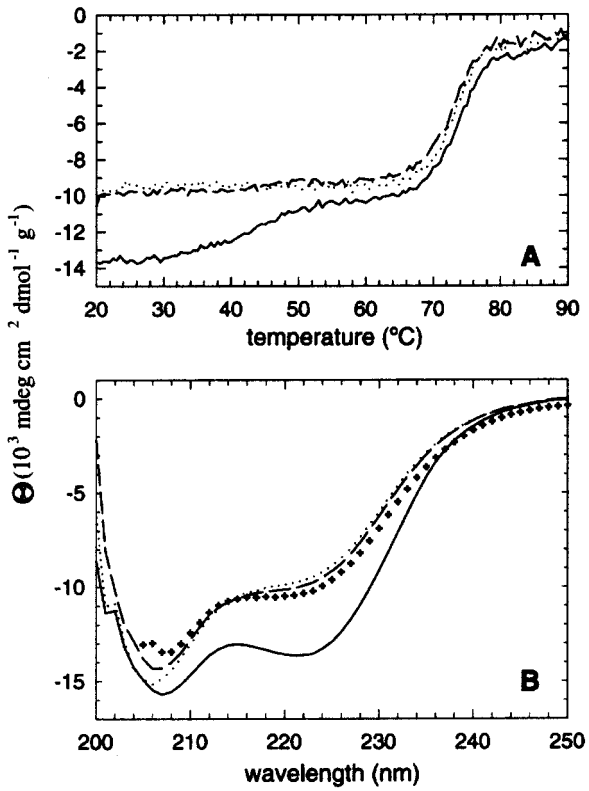

FIGURE 6: Alterations in the secondary structure of KSHV Pr upon point mutation within the dimer interface correlate with the monomer−dimer transition of the active enzyme. (A) Temperature dependence of ellipticity at 222 nm for these forms of KSHV Pr. Only the dimer form of KSHV Pr S204G (solid) has a low-temperature transition, while the mutants, M197D (dashed) and L196A (dotted), appear to exhibit wild-type global stability, denaturing at 75 °C, indicating that the global structural properties of the monomer form of KSHV Pr are unaffected by substitution at the dimer interface. (B) CD spectra of 2.5 μM KSHV Pr S204G, M197D/SG and L196A/SG at 20 °C (labeled as in Figure 5) and 55 °C (crosses). (Note: at 55 °C the signal below 205 nm was out of the linear range of the spectrophotometer's detector, so only data from 205 to 250 nm is plotted). The large difference in spectral shape between monomeric and dimeric KSHV Pr at the lower temperature is dramatically reduced upon temperature elevation. KSHV Pr S204G/M197K behaved identically to the other dimer interface variants in similar, independent assays.

inactive KSHV Pr variants had similar CD spectra (Figure 6B). The active, dimeric KSHV Pr S204G had a much more pronounced spectral minimum at 222 nm (Figure 6B), indicating a different degree of secondary structure content in the dimeric state. At 55 °C, where KSHV Pr S204G exhibited minimal activity, its CD spectrum overlaid closely with that of all the inactive dimer interface protease variants at 20 °C, which did not change their shape or spectral minima from low to high temperature (Figure 6B). These data, taken together, indicate that the secondary structures, including regions near the dimer interface, of KSHV Pr S204G monomers and the M197D and L196A dimer interface variants were similar.

As an independent spectroscopic probe of possible protein conformational changes, fluorescence emission spectra of the inactive dimer interface variants were also collected as a function of temperature and compared to that of KSHV Pr S204G (Figure 7). The spectrum of KSHV Pr S204G at 55 °C, a temperature at which it is inactivated and monomeric (as seen in Figure 3), overlays quite well with the essentially

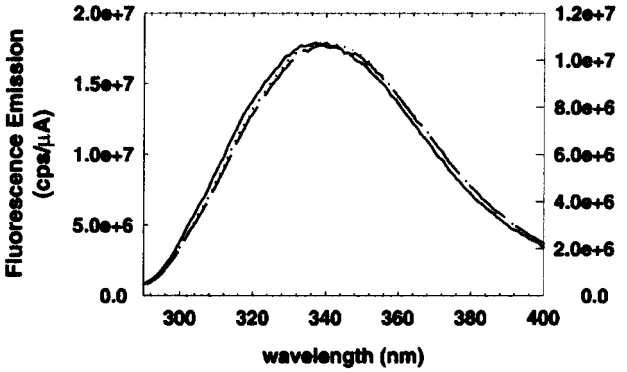

FIGURE 7: Deactivating dimer interface substitutions within KSHV Pr mimic the fluorescence emission spectrum of heat-inactivated monomers of the active enzyme. Fluorescence emission spectra were collected as in Figure 3. At 20 °C the emission spectra of KSHV Pr S204G/L196A (dotted) and S204G/M197D (dashed) overlay with the spectrum of KSHV Pr S204G (solid) at 55 °C. The wavelength of peak emission for all of the 2.5 μM samples was 339 nm. The emission intensity was lower for the KSHV Pr S204G sample due to the higher temperature, therefore it has been scaled to offer better comparison with the spectral shapes of the monomeric proteins' profiles. KSHV Pr S204G/M197K behaved identically to the other dimer interface variants in similar, independent assays.

unchanging spectral shape and emission peak of 339 nm of the stably monomeric protease variants at 20 °C (Figure 7) and at 55 °C, which did not show any shift in spectral position over this temperature range (not shown, for the purpose of clarity). This indicated that the overall tertiary fold and tryptophan solvent exposures of the dimer interface variants resembled that of dissociated monomers of active KSHV Pr S204G.

Modulation of KSHV Pr Dimerization and Activity by Autolysis during Virus Replication. Although the conformational changes that occur in vitro upon monomer → dimer assembly and KSHV Pr D-site cleavage have been documented here and previously (*19*), the linkage between these biophysical studies and the in vivo milieu of a KSHV-infected cell has not been elucidated. To detect the presence of KSHV Pr and/or KSHV Pr Δ during the viral life cycle, KSHV capsids were harvested from latently infected BCBL-1 cells (*25*) and analyzed by Western immunoblot. KSHV undergoes lytic reactivation in these cells upon treatment with the phorbol ester TPA, which induces viral late gene expression, including the protease-assembly protein (Pr/AP) precursor gene (*25*, *29*). Because of the expression of catalytic amounts of the enzyme, as well as the localization of the protease to viral capsid and/or procapsid structures, KSHV Pr was not detected by Western blot analysis of whole cell lysates from induced BCBL-1 cells (unpublished observations). To enrich for the protease molecule in an infected cell culture, the presence of KSHV Pr in released capsid and/or viral particles was then tested. These species were isolated and partially purified from the conditioned media of an induced BCBL-1 culture to determine their protease content. Not only was the presence of KSHV Pr confirmed, the production of KSHV Pr Δ was evident (Figure 8A), indicating that KSHV Pr D-site cleavage occurs either during or after virus assembly and maturation. In addition, it indicated the presence of KSHV Pr and/or KSHV Pr Δ in an infectious viral pool.

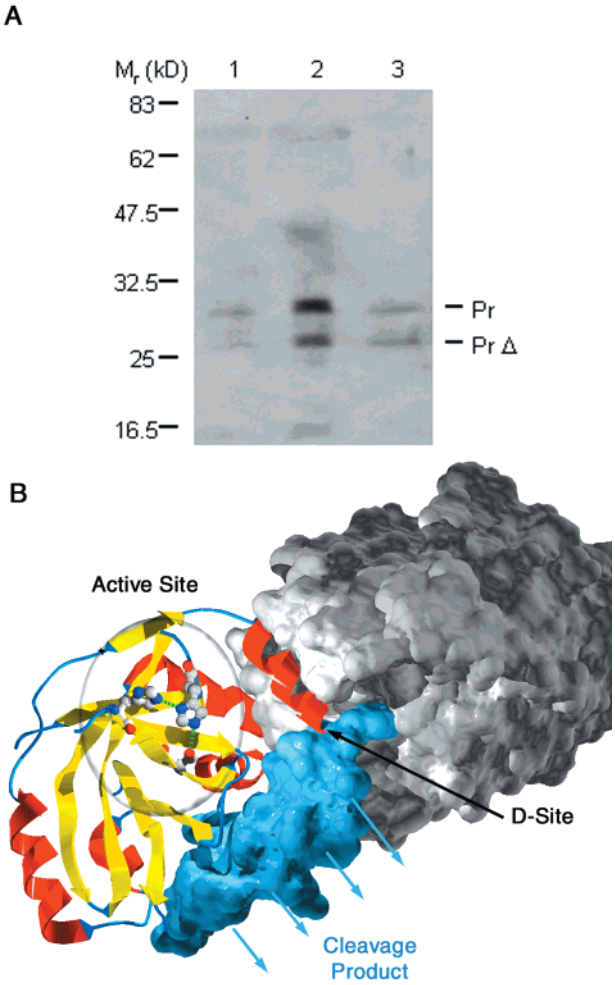

FIGURE 8: Autolysis of KSHV Pr within its dimer interface during viral replication. (A) Detection of KSHV Pr D-site cleavage by western immunoblotting of partially purified viral particles/capsids from the media fraction of TPA-induced BCBL-1 cells. Lanes 1 and 2 contain two different loading volumes of capsid lysate. Lane 3 contains an equimolar mixture of KSHV Pr S204G and KSHV Pr Δ expressed in and isolated from *E. coli*. Cells uninduced with TPA did not produce capsids in sufficient quantity for purification (not shown). (B) Model of the altered molecular surface and loss of dimer interface contacts which occur upon KSHV Pr D-site cleavage. The 27 amino acid fragment, liberated upon D-site cleavage, is depicted in blue with arrows indicating dissociation. To illustrate the loss of contacts upon D-site cleavage an intact monomer is shown in black complexed to the KSHV Pr Δ, shown as a ribbon diagram.

DISCUSSION

While the positive regulatory role of dimerization has been observed previously for the HSV-1, HCMV, and EBV proteases (*22*, *23*, *30*), the presumed and necessary structural coupling has not been elucidated. X-ray crystallographic analyses of proteases from KSHV, HCMV, HSV-1 and -2, and VZV (*5*−*10*) have fostered speculation regarding such allostery. Among the several structures of HCMV, small perturbations (∼5° rotations) of the inter-monomer orientation have been seen upon changes in cosolvent, suggesting a pliant dimer interface. When comparing the herpesviral protease structures, the tertiary packing of the dimer interface exhibits the greatest structural diversity (*5*). A possible mechanism for the stimulation of herpesviral protease activity upon dimerization is through a structural transition in the

interface α-helices, which transmits a structural signal to the molecule's two otherwise independent active sites.

In this study, experimental data are presented supporting the hypothesis that a structural change, centered on the dimer interface and transmitted throughout KSHV Pr, is driven by the protease's self-association. The concentration- and temperature-dependent activity of KSHV Pr agrees well with the CD and fluorescence spectral properties of the enzyme, in the absence of substrate, under identical cosolvent conditions. CD temperature scans of KSHV Pr identify two distinct structural transitions. A high temperature (75 °C) transition appears to be the global unfolding of the KSHV Pr monomers. A lower temperature (∼40 °C) transition coincides with the loss of enzyme activity. The inflection temperature for this deactivation obeys a concentration dependent stabilization of the active species: 40 °C at 2.5 μM vs 34 °C at 250 nM. We have shown here separately that the activity profile of KSHV Pr agrees well with a model in which only dimers are active. Thus, we have detected a structural transition associated with monomerization and deactivation of the protease.

Cleavage at the D-site, seen in vitro in past studies and in vivo here, provides a benchmark for the extent of this structural transition. KSHV Pr efficiently recognizes and cleaves only linear, extended substrates (P4 to P4′); therefore, pursuant to autolysis at the D-site, the dimer interface helix must shift into an extended conformation cleavable in trans by the enzyme. This suggests that at least the last turn of the interface helix unwinds upon dissociation of KSHV Pr dimers. D-site cleavage leads to the irreversible inactivation of KSHV Pr in vitro (*19*) and in viral particles isolated here from a KSHV cell culture model. Free, full-length KSHV Pr monomers may serve as a reversible conformational stopping point in protease deactivation, prior to irreversible D-site cleavage and KSHV Pr Δ production in vivo. The control of the transitions of dimer ↔ monomer and of Pr → Pr Δ may be critical for the proper timing of KSHV Pr activation and deactivation, and thus for virus assembly, maturation and viability as a whole.

Predominantly dimeric under standard conditions, KSHV Pr S204G is ill-suited for the study of the monomer. To provide reagents for study of the KSHV Pr monomer, the dimer interface was targeted for mutagenesis at residues 196 and 197: M197D or K, and L196A. All variants were monomeric and inactive over the concentration ranges accessible to our assays. M197D and M196A exhibited the same global stability in CD temperature scans as our wild-type enzyme (T_M = 75 °C) without the low-temperature transition. Fluorescence emission experiments targeting the tryptophan residues show that the engineered monomers have an indistinguishable emission profile from that of our wild type above its dissociation temperature (55 °C). This profile did not change for the engineered monomers at lower temperatures (20 °C), but did change for wild type as the enzyme passed through its dissociation temperature (∼40 °C). The shift in emission spectrum indicates an increased solvent exposure of the tryptophans in the monomeric species. Trp109, the only tryptophan near the dimer interface, thus appears to be more solvent exposed in the monomer. A greater solvent exposure of the hydrophobic dimer interface in the monomer agrees with the cosolvent activation we observed in this study. Increasing the ionic strength of the assay buffer to 700 mM potassium phosphate favored dimers of wild-type enzyme by ∼1−2 kCal/Mol (K_d of 585 nM vs 1.7 μM). Monomeric variants of the protease characterize the dimer interface to be more solvent exposed and represent molecules for future structural studies of the KSHV Pr interface conformational changes.

This study is not the first to note the structural plasticity of a herpesviral protease. HCMV Pr dimers have been observed to undergo changes in their intrinsic tryptophan fluorescence and the aromatic component of their CD spectra upon binding to a peptidomimetic inhibitor spanning the S4 to S1′ binding pockets (*20*). This fluorescence shift suggests a burial of HCMV-Trp42, a tyrosine in KSHV Pr, upon inhibitor binding. Comparison of apo and inhibitor-bound HCMV structures show the ordering of residues around Trp42, distal to the dimer interface. A possible active site to dimer interface linkage has been seen in HCMV Pr. The structure of HCMV Pr bound to an inhibitor exhibits a small reorganization of the monomers at the dimer interface, although cooperative substrate/inhibitor binding and/or hydrolysis has not been reported in the literature for any herpesviral protease, or seen by us with KSHV Pr (unpublished observations). The more pronounced spectroscopic differences seen in this study of KSHV Pr dimerization indicate that larger conformational changes take place during self-association than during inhibitor binding. As this paper was under review, a report was published describing the structure of dimeric HCMV Pr containing mutations at selected dimer interface positions (*34*). These variants exhibited altered monomer structures within the dimer. This study, by isolating a significantly less active dimeric structural intermediate, provides structural evidence that alterations within the dimer interface influence the secondary structure of regions distal to the interface and thus the activity of herpesviral proteases. Taken together with our studies of the monomer structure, the above findings suggest a structural pathway in which the dimer interface and C-terminal helices and functionally associated active-site residues lose structural coherence along the transition from active dimers to the inactive monomers.

Herpesviral proteases provide an interesting case study for the allosteric transitions that order active site and/or substrate binding determinants upon dimerization of proteases. Other proteases characterized to date undergo a controlled activation process (*24*). This process, normally performed utilizing an N-terminal propeptide release mechanism, induces order in, and/or releases a blocking motif from, the enzyme's active site. Herpesviral proteases, on the other hand, do not have such zymogen activation sequences, but rather are expressed with C-terminal scaffold molecule fusions, and thus must use a different mechanism of activation. The current and past structural studies on herpesviral proteases have been performed in the absence of its cotranslationally expressed substrate, the viral scaffold AP molecule. The allosteric properties (during dimerization and D-site cleavage) of KSHV Pr would become the control mechanism upon release of KSHV Pr from the polyprotein. It has been recently demonstrated that HSV-1 Pr is selectively maintained in mature virus particles even though its substrate molecule, the viral scaffolding protein, is removed prior to viral DNA packaging (*35*). In light of the detection of KSHV Pr in virions and/or viral procapsids, it is possible that this viral

protease may function in an analogous manner in KSHV, and that KSHV Pr Δ may play some structural and/or functional role in the virion, highlighting the critical role of the herpesviral dimer interface in its allosteric regulation.

ACKNOWLEDGMENT

The authors thank Profs. Don Ganem and Michael Lagunoff for resources and advice regarding KSHV tissue culture and purification. We also thank Prof. Robert Stroud for support and advice regarding structural aspects of KSHV Pr, as well as Anson Nomura and Alan Marnett for their comments and critical reading of the manuscript.

REFERENCES

1. Russo, J. J., Bohenzky, R. A., Chien, M. C., Chen, J., Yan, M., Maddalena, D., Parry, J. P., Peruzzi, D., Edelman, I. S., Chang, Y., and Moore, P. S. (1996) *Proc. Natl. Acad. Sci. U.S.A. 93*, 14862−14867.
2. Ganem, D. (1997) *Cell 91*, 157−160.
3. Roizmann, B., and Sears, A. E. (1996) in *Virology* (Fields et al., Ed.) pp 2231−2295, Lippincott-Raven, New York.
4. Gibson, W. (1996) *Intervirology 39*, 389−400.
5. Reiling, K. K., Pray, T. R., Craik, C. S., and Stroud, R. M. (2000) *Biochemistry 39*, 12796−803.
6. Tong, L., Qian, C., Massariol, M., Bonneau, P., Cordingley, M. G., and Lagacé, L. (1996) *Nature 383*, 272−275.
7. Qiu, X., Culp, J. S., DiLella, A. G., Hellmig, B., Hoog, S. S., Janson, C. A., Smith, W. W., and Abdel-Meguid, S. S. (1996) *Nature 383*, 275−279.
8. Shieh, H., Kurumbail, R. G., Stevens, A. M., Stegeman, R. A., Sturman, E. J., Pak, J. Y., Wittwer, A. J., Palmier, M. O., Wiegand, R. C., Holwerda, B. C., and Stallings, W. C. (1996) *Nature 383*, 279−282.
9. Chen, P., Tsuge, H., Almassy, R. J., Gribskov, C. L., Katoh, S., Vanderpool, D. L., Margosiak, S. A., Pinko, C., Matthews, D. A., and Kan, C. (1996) *Cell 86*, 835−843.
10. Qiu, X., Janson, C. A., Culp, J. S., Richardson, S. B., Debouck, C., Smith, W. W., and Abdel-Meguid, S. S. (1997) *Proc. Natl. Acad. Sci. U.S.A. 94*, 2874−2879.
11. Hoog, S. S., Smith, W. W., Qiu, X., Janson, C. A., Hellmig, B., McQueney, M. S., O'Donnell, K., O'Shannessy, D., DiLella, A. G., Debouck, C., and Abdel-Meguid, S. S. (1997) *Biochemistry 36*, 14023−14029.
12. Hosfield, C. M., Elce, J. S., Davies, P. L., and Jia, Z. (1999) *EMBO J. 18*, 6880−9.
13. Joshua-Tor, L., Xu, H. E., Johnston, S. A., and Rees, D. C. (1995) *Science 269*, 945−50.
14. Sommerhoff, C. P., Bode, W., Matschiner, G., Bergner, A., and Fritz, H. (2000) *Biochim. Biophys. Acta 1477*, 75−89.
15. Tamura, T., Tamura, N., Cejka, Z., Hegerl, R., Lottspeich, F., and Baumeister, W. (1996) *Science 274*, 1385−9.
16. Chen, P., and Hochstrasser, M. (1996) *Cell 86*, 961−72.
17. Wlodawer, A., Miller, M., Jaskolski, M., Sathyanarayana, B. K., Baldwin, E., Weber, I. T., Selk, L. M., Clawson, L., Schneider, J., and Kent, S. B. (1989) *Science 245*, 616−621.
18. Navia, M. A., Fitzgerald, P. M., McKeever, B. M., Leu, C. T., Heimbach, J. C., Herber, W. K., Sigal, I. S., Darke, P. L., and Springer, J. P. (1989) *Nature 337*, 615−620.
19. Pray, T. R., Nomura, A. M., Pennington, M. W., and Craik, C. S. (1999) *J. Mol. Biol. 289*, 197−203.
20. Bonneau, P. R., Grand-Maitre, C., Greenwood, D. J., Lagace, L., LaPlante, S. R., Massariol, M.-J., Ogilvie, W. W., O'Meara, J. A., and Kawai, S. H. (1997) *Biochemistry 36*, 12644−12652.
21. Tong, L., Qian, C., Massariol, M. J., Déziel, R., Yoakim, C., and Lagacé, L. (1998) *Nat. Struct. Biol. 5*, 819−826.
22. Darke, P. L., Cole, J. L., Waxman, L., Hall, D. L., Sardana, M. K., and Kuo, L. C. (1996) *J. Biol. Chem. 271*, 7445−7449.
23. Schmidt, U., and Darke, P. L. (1997) *J. Biol. Chem. 272*, 7732−7735.
24. Khan, A. R., and James, M. N. (1998) *Protein Sci. 7*, 815−36.
25. Renne, R., Zhong, W., Herndier, B., McGrath, M., Abbey, N., Kedes, D., and Ganem, D. (1996) *Nat. Med. 2*, 342−6.
26. Holskin, B. P., Bukhtiyarova, M., Dunn, B. M., Baur, P., de Chastonay, J., and Pennington, M. W. (1995) *Anal. Biochem. 227*, 148−155.
27. Kleywegt G. J.; Jones T. A. (1994) *ESF/CCP4 Newsletter 31*, 9−14.
28. Hall, D. L., and Darke, P. L. (1995) *J. Biol. Chem. 270*, 22697−700.
29. Ünal, A., Pray, T. R., Lagunoff, M., Pennington, M. W., Ganem, D., and Craik, C. S. (1997) *J. Virol. 71*, 7030−7038.
30. Buisson, M., Valette, E., Hernandez, J. F., Baudin, F., Ebel, C., Morand, P., Seigneurin, J. M., Arlaud, G. J., and Ruigrok, R. W. (2001) *J. Mol. Biol. 311*, 217−28.
31. Waxman, L., and Darke, P. L. (2000) *Antivir. Chem. Chemother. 11*, 1−22.
32. Fersht, A. (1985) *Enzyme Structure and Mechanism*, 2nd ed., W. H. Freeman, New York.
33. Cantor, C. R., and Schimmel, P. R. (1980) *Biophysical Chemistry*, W. H. Freeman and Co., New York.
34. Batra, R., Khayat, R., and Tong, L. (2001) *Nat. Struct. Biol. 8*, 810−817.
35. Sheaffer, A. K., Newcomb, W. W., Brown, J. C., Gao, M., Weller, S. K., and Tenney, D. J. (2000) *J. Virol. 74*, 6838−6848.

BI011753G